

Disrupting bonding in azoles through beryllium bonds: Unexpected coordination patterns and acidity enhancement

Cite as: J. Chem. Phys. **156**, 194303 (2022); <https://doi.org/10.1063/5.0089716>

Submitted: 28 February 2022 • Accepted: 26 April 2022 • Accepted Manuscript Online: 26 April 2022 • Published Online: 16 May 2022

 M. Merced Montero-Campillo,  Otilia Mó,  Ibon Alkorta, et al.

COLLECTIONS

Paper published as part of the special topic on [Nature of the Chemical Bond](#)



View Online



Export Citation



CrossMark

ARTICLES YOU MAY BE INTERESTED IN

[The nature of supermolecular bonds: Investigating hydrocarbon linked beryllium solvated electron precursors](#)

The Journal of Chemical Physics **156**, 194302 (2022); <https://doi.org/10.1063/5.0089815>

[Stereoinversion of tetrahedral p-block element hydrides](#)

The Journal of Chemical Physics **156**, 194113 (2022); <https://doi.org/10.1063/5.0090267>

[The influence of a solvent environment on direct non-covalent interactions between two molecules: A symmetry-adapted perturbation theory study of polarization tuning of \$\pi-\pi\$ interactions by water](#)

The Journal of Chemical Physics **156**, 194306 (2022); <https://doi.org/10.1063/5.0087302>



[Learn More](#)

Special Topics Open for Submissions

Disrupting bonding in azoles through beryllium bonds: Unexpected coordination patterns and acidity enhancement

Cite as: J. Chem. Phys. 156, 194303 (2022); doi: 10.1063/5.0089716

Submitted: 28 February 2022 • Accepted: 26 April 2022 •

Published Online: 16 May 2022



M. Merced Montero-Campillo,¹ Otilia Mó,¹ Ibon Alkorta,² José Elguero,² and Manuel Yáñez^{1,a)}

AFFILIATIONS

¹ Departamento de Química, Módulo 13, Facultad de Ciencias and Institute for Advanced Research in Chemical Sciences (IAdChem), Universidad Autónoma de Madrid, Madrid 28049, Spain

² Instituto de Química Médica (CSIC), Juan de la Cierva, 3, E-28006 Madrid, Spain

Note: This paper is part of the JCP Special Topic on Nature of the Chemical Bond.

^{a)} Author to whom correspondence should be addressed: manuel.yanez@uam.es

ABSTRACT

Although triazoles and tetrazole are amphoteric and may behave as weak acids, the latter property can be hugely enhanced by beryllium bonds. To explain this phenomenon, the structure and bonding characteristics of the complexes between triazoles and tetrazoles with one and two molecules of BeF₂ have been investigated through the use of high-level G4 *ab initio* calculations. The formation of the complexes between the N basic sites of the azoles and the Be center of the BeF₂ molecule and the (BeF₂)₂ dimer leads to a significant bonding perturbation of both interacting subunits. The main consequence of these electron density rearrangements is the above-mentioned increase in the intrinsic acidity of the azole subunit, evolving from a typical nitrogen base to a very strong nitrogenous acid. This effect is particularly dramatic when the interaction involves the (BeF₂)₂ dimer, that is, a Lewis acid much stronger than the monomer. Although the azoles investigated have neighboring N-basic sites, their interaction with the (BeF₂)₂ dimer yields a monodentate complex. However, the deprotonated species

becomes extra-stabilized because a second N–Be bond is formed, leading to a new $\text{N}-\text{N}-\text{Be}-(\text{F}_2)-\text{Be}$ five-membered ring, with the result that the azole-(BeF₂)₂ complexes investigated become stronger nitrogenous acids than oxyacids such as perchloric acid.

© 2022 Author(s). All article content, except where otherwise noted, is licensed under a Creative Commons Attribution (CC BY) license (<http://creativecommons.org/licenses/by/4.0/>). <https://doi.org/10.1063/5.0089716>

INTRODUCTION

Almost since the origins of quantum chemistry, it was clear that what we call a chemical bond was not a quantum mechanically defined property.¹ However, it became also more and more evident that a fundamental understanding of this basic concept requires a rigorous quantum mechanical treatment of the whole system.² Even more importantly, all along the last decades of the past century and the first decades of the present one, the concept of bonding was behind the birth of a plethora of new techniques, both experimental and theoretical. A very interesting and beautiful analysis of the concept of bond was published by Ball a decade ago, where its contradictions and elusive nature all along history are discussed.³

It is also quite obvious that many molecular properties, such as bond lengths, or bond dissociation energies, are related to the

strength of the chemical bonds. The internuclear electron density, which is a well-defined magnitude, offers important information about the characteristics of the interactions between the atoms of a system. As a matter of fact, through the derivatives of the electron density, it is possible to establish the reaction paths where chemical bonds are breaking and forming,^{4,5} and the on-top pair density can provide interesting insight into bond breaking.⁶ In addition, the analysis of the deformation of the electron density provides interesting insights into chemical binding.⁷ The electron density allowed as well to detect and characterize different kinds of non-covalent interactions, such as dihydrogen,⁸ beryllium,⁹ pnictogen,¹⁰ or tetrel bonds.¹¹ Electron density is again crucial when analyzing and characterizing cooperative or anti-cooperative effects when two or more non-covalent interactions, among them beryllium bonds, coincide in the same system.^{12–31} Beryllium bonds, in particular,

have been shown to be crucial in ring expansion reactions involving cyclic(alkyl)(amino) carbenes.³² It should be remarked that the analysis of the electron density allows us to identify how and how much intermolecular interactions alter the bonding within each of the interacting units and modify their intrinsic reactivity. Likely, the first example in which this phenomenon was experimentally confirmed was the acidity enhancement of phosphines when associated with boranes,³³ to the point that the ionization constant increases between 13 and 18 orders of magnitude, which implies an increase of 80–110 kJ mol⁻¹ in terms of intrinsic acidities. Similar enhanced acidities were also predicted for some azoles upon interaction with beryllium derivatives.³⁴ Likewise, a significant acidity enhancement was found for complexes between unsaturated N, P, As, and Sb containing compounds and beryllium dihydride but, quite unexpectedly, it was Be (and not P, As, and Sb) that behaved as a Brønsted acid.³⁵ Along these lines, it was also found, through the use of high-level *ab initio* calculations, that the complexes between unsaturated hydrocarbons, such as ethylene and acetylene, with beryllium dichloride are acids as strong as nitric and sulfuric acids, respectively, whereas 1*H*-tetrazole–BeCl₂ is a nitrogen acid stronger than an oxyacid such as perchloric acid.³⁶

The aim of this paper is to try to get a reasonable answer to some interesting questions arising from those findings that, to the best of our knowledge, have not been addressed yet. One is what would be the behavior of bases such as triazoles and tetrazoles, with more than one basic site, if they interact with two rather than with one beryllium derivative. Of course, it can be easily anticipated that when we are dealing with only one beryllium derivative, the attachment would preferentially occur at the most basic N site; however, it is not so obvious when the number of attacking Be derivatives is two. Do the Be molecules attach to two different basic sites? Do they on the contrary form a dimer before attaching to the azole molecule? How intense are the bonding perturbations in the azole unit in these cases? What is the acidity enhancement of the azole unit? To get this information, we have carried out high-level *ab initio* calculations on 1*H*- and 2*H*-1,2,3-triazole, 1*H*- and 4*H*-1,2,4-triazole, and 1*H*- and 2*H*-tetrazole as well when interacting with one and two beryllium difluoride molecules.

COMPUTATIONAL DETAILS

Since the accuracy in the calculation of acidity enhancements and the analysis of the bond perturbations is crucial to obtain reliable conclusions, we have used for our study the composite *ab initio* Gaussian-4 (G4) theory,³⁷ which, in general, provides thermochemistry magnitudes with an average absolute deviation from experiment of 3.47 kJ mol⁻¹. The use of this methodology is also advisable because we are dealing with non-covalent interactions for which the binding energies are much smaller than those of conventional chemical bonds and, therefore, the errors in obtaining them should be reduced as much as possible. In this composite method, the equilibrium structures and the harmonic vibrational frequencies are obtained at the B3LYP/6-31G(2df, p) level of theory. The G4 method yields final energies very close to those obtained in a formal CCSD(T,full)/G3LargeXP calculation but employs a composite procedure in which the different energy components to obtain the final value are obtained at MP2, MP4,^{38,39} and CCSD(T)⁴⁰ levels of theory, with a final correction evaluated at the Hartree–Fock limit.

A possible reluctance to use this model, when applied to weak non-covalent interactions, is the use of B3LYP optimized geometries. To verify if this was, indeed, an issue, we have chosen the most stable complexes of 1*H*-1,2,3-triazole and 1*H*-tetrazole with one and two BeF₂ molecules as representative systems to carry out G4 calculations (that will be named G4* calculations) using ω B97XD optimized geometries rather than the B3LYP ones. The results obtained (see Fig. S1 and Table S1 of the [supplementary material](#)) show that the changes in the optimized geometries when changing the functional are really small, but what is more important the changes in the binding enthalpies (between 0.1 and 2.2 kJ mol⁻¹) are not significant.

As mentioned in the Introduction, it is the electron density that regulates the strength of the bonds and the intensity of the non-covalent interactions, hence we have paid particular attention to its analysis using three complementary methodologies, the Quantum Theory of Atoms in Molecules (QTAIM),⁴¹ the electron density shifts (EDS),⁴² and the Electron Localization Function (ELF).⁴³ In all cases, we have used the same level of theory [B3LYP/6-31G(2df,p)] as the one employed in the G4 formalism for the geometry optimization. The QTAIM method proposed by Bader in 1990 analyses the topology of the electron density of the system by locating its critical points. Particularly relevant to determine the strength of the chemical bonds within the system are the bond critical points (BCPs), whose electron density, $\rho(\mathbf{r})$, provides useful information on the relative strength of the bond in which it is located. The EDS is particularly useful to analyze the strength and characteristics of non-covalent interactions because it is obtained as the difference between the electron density of the intermolecular complex and the isolated components with the geometry they have in the complex. In this way, it is possible to locate those areas of the complexes in which an electron density shift from one subunit to another takes place as a consequence of the complex formation.⁴⁴ The ELF is a 3D scalar function that allows finding regions of the space of high electronic localization where the Pauli repulsion is low. These regions or basins, which can be identified with lone pairs, bonds, and atom cores, are characterized by a low value of the excess local kinetic energy, which is the difference between the local kinetic energy of a non-interacting bosonic system and a fermionic one. These basins are named monosynaptic basins when associated with a single atom (core, lone pairs) and disynaptic (or polysynaptic) when associated with two or more atoms, corresponding to bonding pairs. Finally, the molecular electrostatic potential (MESP) of the isolated 1*H*-1,2,3-triazole was obtained to identify the electron-deficient and electron-rich areas of the system with the GAUSSIAN package,⁴⁵ analyzed on the 0.001 e/bohr³ electron density isosurface with the Multiwfn program⁴⁶ and represented with Jmol.⁴⁷

RESULTS AND DISCUSSION

In our theoretical survey of the interaction of triazoles and tetrazoles with one and two molecules of BeF₂, we have considered each and every one of the possible associations depending on the N basic centers available in each azole.

Complexes azole–BeF₂

The complexes found to be a minimum of the corresponding potential energy surface when the interaction involves only

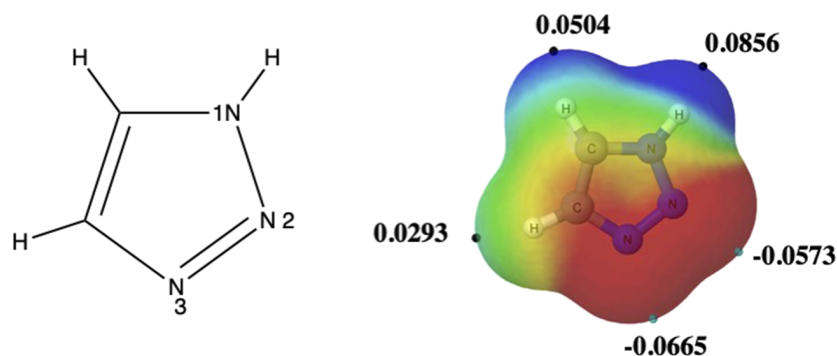


FIG. 1. Molecular electrostatic potential map of 1H-1,2,3-triazole. Black and green dots correspond to maxima and minima, respectively. Potential values are in a.u.

one BeF₂ molecule are shown in Figs. S2–S5 of the [supplementary material](#). Moreover, in these figures, we provide the BeF₂ binding enthalpies for each complex, its intrinsic acidity, which is one of the intrinsic properties that changes more dramatically. For the sake of conciseness, we are going to discuss in detail only the

cases of the 1H- and 2H-1,2,3-triazole from the family of triazoles and 1H-tetrazole from the family of tetrazoles as illustrative examples.

The N2 and N3 centers of 1H-1,2,3-triazole are the potential basic sites of this azole and attending to the characteristics of its

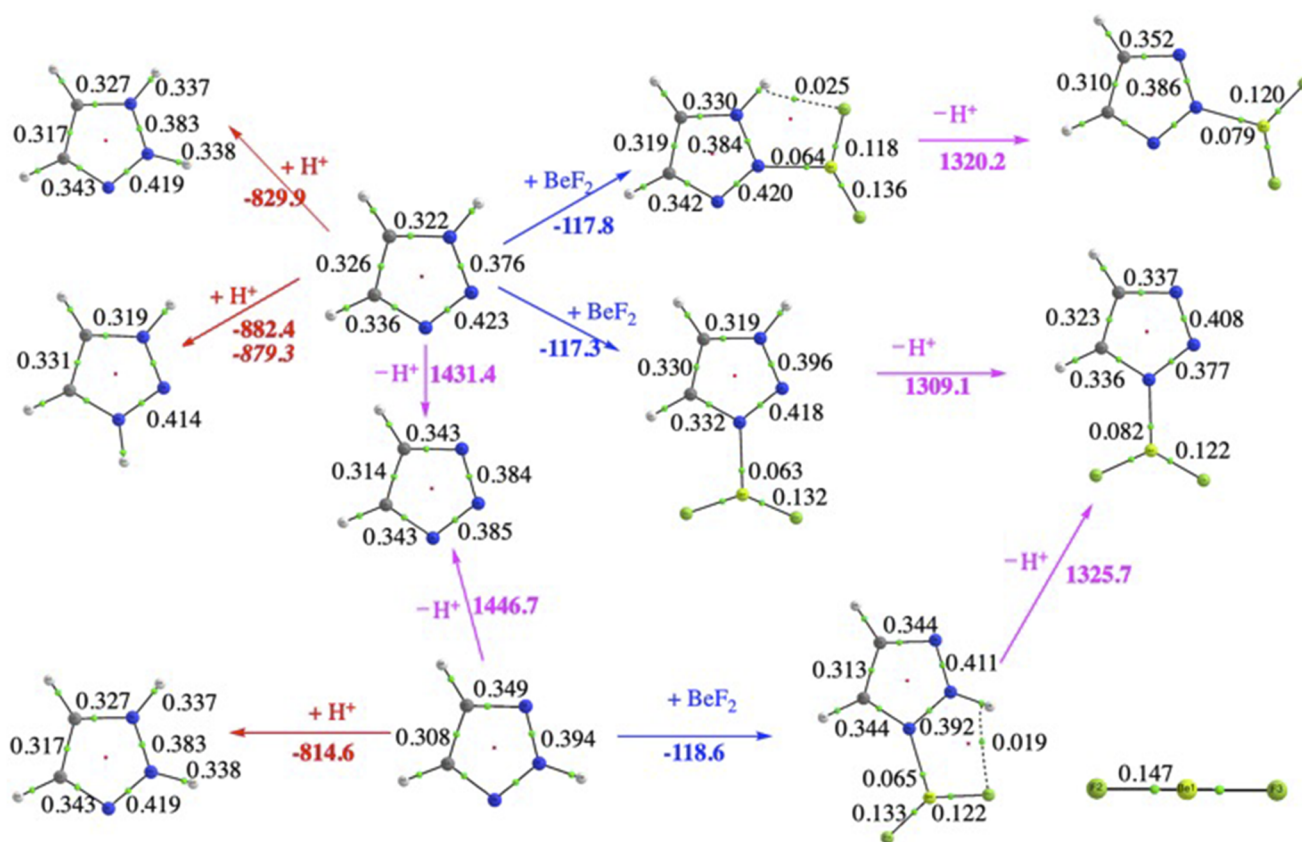


FIG. 2. Scheme showing the energetics and molecular graphs corresponding to different processes with origin in 1H- and 2H-1,2,3-triazoles. Red, magenta, and blue arrows identify protonation, deprotonation, and BeF₂ association processes. The associated numerical values correspond to -PAs, intrinsic acidities, and BeF₂ binding enthalpies, respectively, in kJ mol⁻¹. Red cursive numbers denote the experimental PA of 1H-1,2,3-triazole. The molecular graph of the BeF₂ molecule is given at the low right corner. The molecular graphs include the electron densities (a.u.) at the corresponding BCPs.

molecular electrostatic potential (see Fig. 1) one would expect N3 to be the most favorable site for an electrophilic interaction, in agreement with previous theoretical and experimental studies.^{48,49}

Indeed, as illustrated in Fig. 2, the calculated proton affinity (PA)⁵⁰ for this center, which agrees very well with the experimental PA of 1*H*-1,2,3-triazole (879.3 kJ/mol), is 52.5 kJ mol⁻¹ higher than the PA of N2. One would expect, naively, that N3 should also be the preferential site for BeF₂ association, since the formation of the N–Be bond implies an electron density transfer from the basic site of the azole to the empty *p* orbital of the BeF₂ molecule, very much the same as the transfer to the incoming proton when the system becomes protonated. This implies the *sp*^{*n*} Be orbitals in isolated BeF₂ to evolve to *sp*^{*n*} (1 < *n* ≤ 2) in the complex, with F–Be–F bond angles much smaller than 180° (typically in the range of 137°–140°). In addition, consistently with this scenario, both protonation and BeF₂ association should lead to similar electron density redistributions within the five-membered ring. As revealed by the density values on the BCPs in Fig. 2, when the active site is N2, the N1–N2, N3–C4, and C5–N1 bonds become reinforced, and the N2–N3 and C4–C5 bonds weaken. If the association takes place at N3, only N1–N2 and C4–C5 bonds reinforce. However, the molecular graph of the N2 complex clearly shows the existence of a second non-covalent stabilizing interaction in the form of a N–H···F intramolecular hydrogen bond (IMHB) that extra-stabilizes this complex with respect to the one in which the BeF₂ molecule is attached to N3 where no IMHB is formed. The consequence is that the BeF₂ binding enthalpy to N3

is not larger but practically equal (a difference of 0.5 kJ mol⁻¹) to the binding enthalpy to N2. A similar IMHB also explains the fact that whereas 1*H*-1,2,3-triazole has a PA of 67.8 kJ mol⁻¹ higher than its isomer 2*H*-1,2,3-triazole, the BeF₂ binding energy of the latter is slightly larger than that of the former (118.6 vs 117.8 kJ mol⁻¹).

Figure 2 also shows the dramatic changes in the electron densities of the azole-BeF₂ complexes when they become deprotonated. The increase in the global electron density of the azole moiety upon the loss of the proton is reflected in a significant increase in the electron density transfer to the BeF₂ molecule. For the 1*H*-1,2,3-triazole, this increase is about 30% of the electron density at the N–Be BCP, this effect being stronger when BeF₂ is attached to N3 (from 0.063 to 0.082 a.u.) than when it is attached to N2 (from 0.064 to 0.079 a.u.) because N3 is intrinsically a stronger basic site than N2. Consistently, the N3–Be bond shortens 0.055 Å upon the deprotonation of the triazole. This binding reinforcement is reflected in a huge acidity enhancement (122.3 kJ mol⁻¹) of the azole moiety upon BeF₂ attachment. The consequence is that whereas the isolated 1*H*-1,2,3-triazole molecule is a weak acid, the 1*H*-1,2,3-triazole-BeF₂ complex becomes a rather strong nitrogen acid (1309.1 kJ mol⁻¹) in the gas phase, 74 kJ mol⁻¹ stronger than an oxyacid such as phosphoric acid (1383 ± 21 kJ mol⁻¹),⁵¹ and 48 kJ mol⁻¹ than nitric acid (1357.7 ± 0.84 kJ mol⁻¹).⁵² The existence of the N–H···F IMHB in the 2*H*-1,2,3-triazole-BeF₂ complex, which extra-stabilizes the neutral complex, is responsible for its lower acidity (1325.7 kJ mol⁻¹) with respect to the 1*H*-1,2,3-triazole-BeF₂ analog.

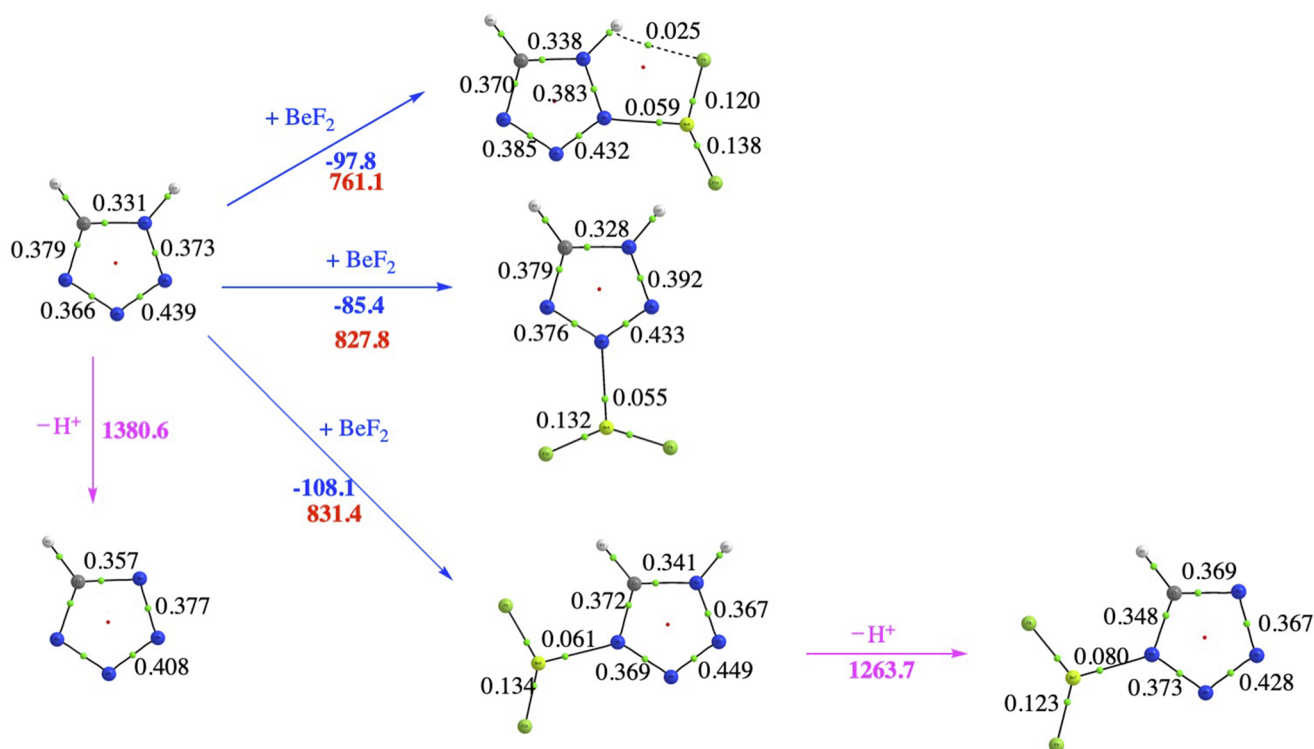


FIG. 3. Scheme showing the energetics and molecular graphs corresponding to the BeF₂ association to 1*H*-tetrazole (blue) and the deprotonation of the 1*H*-tetrazole-BeF₂ complexes (magenta). Same conventions as in Fig. 2.

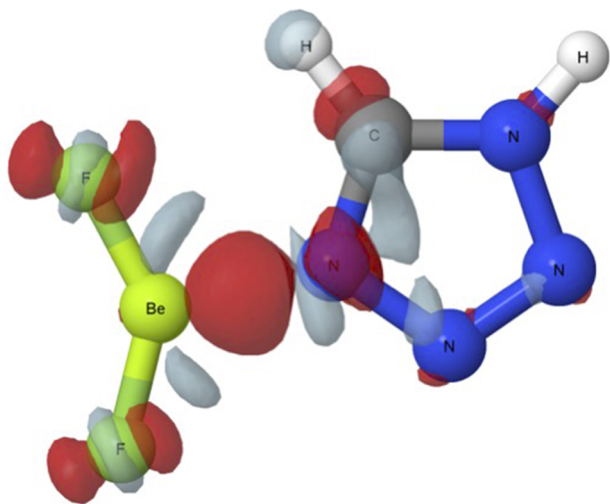


FIG. 4. EDS plot (isosurface ± 0.004 a.u.) for the most stable *1H*-tetrazole- BeF_2 complex. Red lobes correspond to areas in which the electron density is accumulated, whereas gray ones correspond to areas where the electron density is depleted.

Let us now briefly analyze the results for *1H*-tetrazole. In this case, as shown in red numbers in Fig. 3, the gap between the gas-phase basicities at N4 and N2 is very large (70.3 kJ/mol). For this reason, even if the attachment of BeF_2 to N2 is accompanied by the formation of a $\text{N-H} \cdots \text{Be}$ IMHB that does not exist when the attachment takes place at N3 or N4, the N4- BeF_2 complex remains the global minimum.

The EDS plot for the global minimum (see Fig. 4) well illustrates that the region with a preferential accumulation of electron density is precisely between the N4 basic site and the Be atom, giving rise to the corresponding beryllium bond. Also, smaller areas of electron density accumulation appear associated with the F atoms because the richer electron population around Be atom favors some transfer to these very electronegative substituents.

The deprotonation of *1H*-tetrazole- BeF_2 follows a mechanism similar to the one discussed above for *1H*-1,2,3-triazole- BeF_2 complex and leads to the concomitant acidity enhancement. Indeed, Fig. 3 shows that the deprotonation of the most stable *1H*-tetrazole- BeF_2 complex implies a significant reinforcement of the beryllium bond, whose electron density at the BCP increases from 0.061

to 0.080 a.u. Consistently, the ELF approach also reflects this bond reinforcement (see Fig. 5), since the population of the N-Be disynaptic basin increases from 3.12 to 3.32 e^- upon deprotonation. This increase in the electron density transferred to the BeF_2 unit is also reflected in a decrease of the F-Be-F angle from 138.5° in the neutral compound to 127.2° in the anionic deprotonated species. In addition, a bond reinforcement is observed for the two bonds in which the deprotonated NH group participates.

Finally, it should be remarked that, since already *1H*-tetrazole is more acidic than *1H*-1,2,3-triazole (1380.6 vs 1431.4 kJ mol $^{-1}$), the BeF_2 complex of the former is predicted to be not only more acidic than phosphoric or nitric acids but even more acidic than sulfuric acid (1295 ± 23 kJ mol $^{-1}$).⁵³

Complexes azole- $(\text{BeF}_2)_2$

As in the Azole- BeF_2 section, the different complexes found to be a minimum when two molecules of BeF_2 interact with the azoles under investigation, for all possible conformations, as shown in Figs. S6–S10 of the [supplementary material](#). Like for the case where only one BeF_2 molecule was interacting with the azole, the binding enthalpy for each complex and its intrinsic acidity are also given. Following a similar pattern as in the previous section, we are going to discuss in more detail the results obtained for *1H*-1,2,3-triazole and *1H*-tetrazole as suitable examples.

When the interaction involves two rather than only one BeF_2 molecule, we cannot discard the possibility of the dimerization of BeF_2 , where each Be atom acts as a Lewis acid with respect to the fluorine atoms of the other BeF_2 monomer. Indeed, a rather stable $(\text{BeF}_2)_2$ dimer can be formed, as shown in the lower left corner of Fig. 6. Its dimerization energy estimated at the G4 level is 152.6 kJ mol $^{-1}$.

In the same figure, three different association mechanisms are shown. In the first one, each BeF_2 molecule interacts with each of the basic sites of *1H*-1,2,3-triazole, though as clearly indicated by the electron densities at the Be-N bond critical points, the Be-N3 interaction is stronger than the Be-N2, as it should be expected from the higher intrinsic basicity of N3 already mentioned in the Azole- BeF_2 section. It should also be noted that the BeF_2 unit attached to N2 also participates in a $\text{N-H} \cdots \text{F}$ IMHB, which contributes to stabilize this complex. Also, a very weak $\text{F} \cdots \text{F}$ non-covalent interaction between both BeF_2 units is observed. Alternatively, the two BeF_2 molecules may form the $(\text{BeF}_2)_2$ dimer before interacting with the azole. These complexes are significantly more stable than the previous one, and

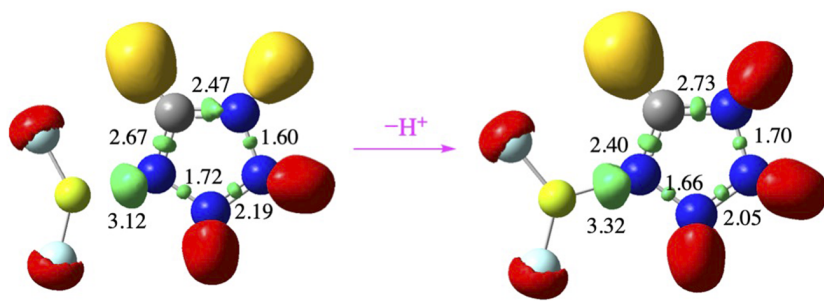


FIG. 5. ELF function, with an isovalue of 0.85, calculated for the most stable *1H*-tetrazole- BeF_2 complex and its deprotonated form. The population of each basin is indicated in electrons. Monosynaptic basins are shown in red and disynaptic in green, except those involving hydrogen atoms (C-H and N-H), which are in yellow.

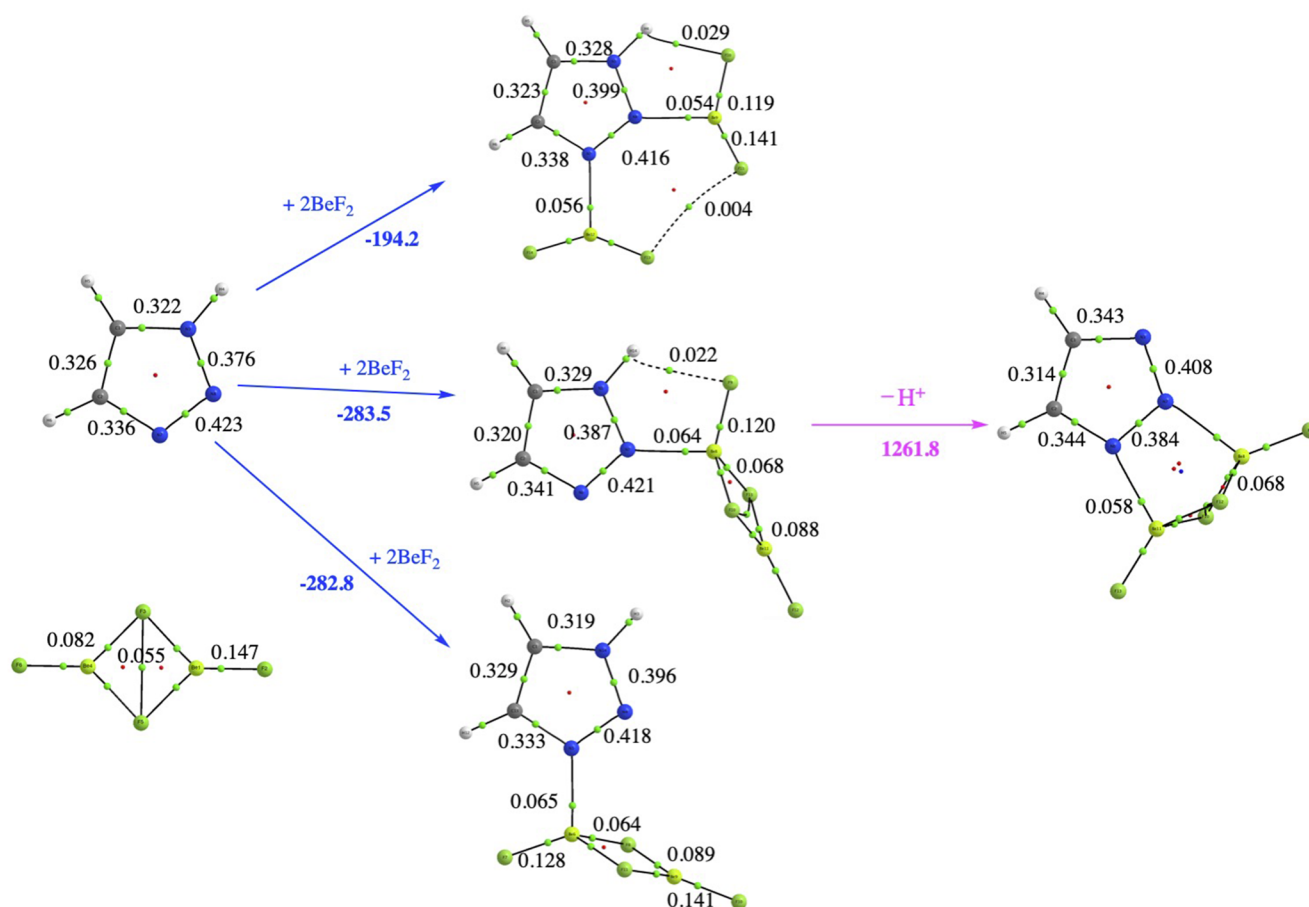


FIG. 6. Scheme showing the energetics and molecular graphs corresponding to the possible ways (binding energies in blue) of interaction between 1H-1,2,3-triazole and two molecules of BeF₂, as well as the deprotonation (magenta) of the most stable 1H-1,2,3-triazole-BeF₂ complex. At the lower left corner, we show the molecular graph of the (BeF₂)₂ dimer. Same conventions as in Fig. 2.

this is a rule (see Figs. S6–S10 of the [supplementary material](#)) for all the azoles envisaged in our study. On top of that, we cannot ignore that (BeF₂)₂ is a stronger Lewis acid than the monomer because in the dimer, each Be atom is bound to three very electronegative F

atoms. Indeed, by comparing the values in Fig. 6 with those in Fig. 2, it can be noted that whereas the binding energies of the monomer are around 117 kJ mol⁻¹ (Fig. 2), for the dimer, they are more than twice (~283 kJ mol⁻¹) this value.

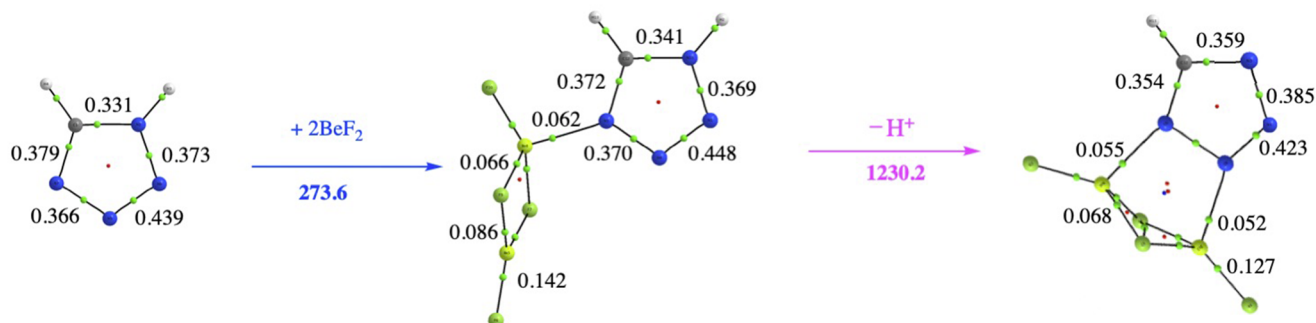


FIG. 7. Scheme showing the formation of the most stable 1H-tetrazole-(BeF₂)₂ complex (blue) and its intrinsic acidity (magenta). Same conventions as in Fig. 2. Note that in the deprotonated system, N1 and N2 are identical to N4 and N3 by symmetry.

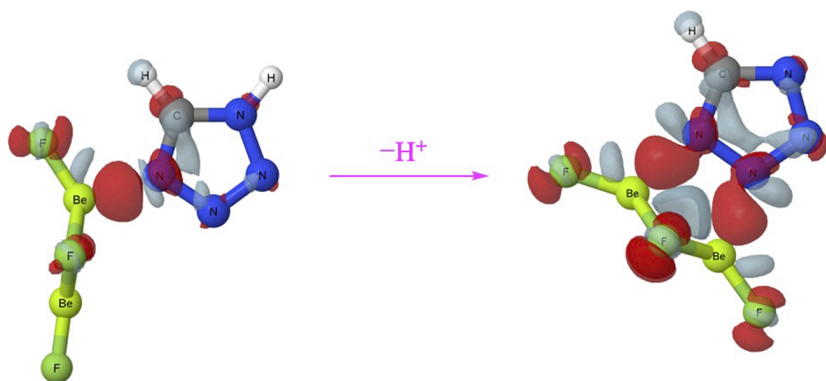


FIG. 8. EDS plot for the most stable 1H-tetrazole-(BeF₂)₂ complex and its deprotonated form. Same conventions as in Fig. 4.

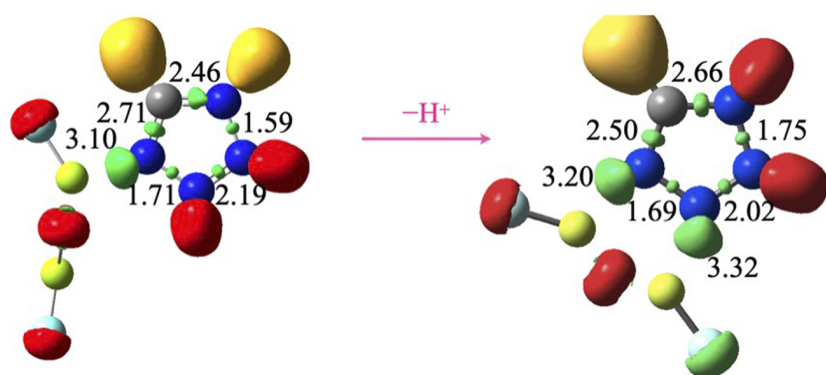


FIG. 9. ELF function, with an isovalue of 0.85, calculated for the most stable 1H-tetrazole-(BeF₂)₂ complex and its deprotonated form. The population of each basin is indicated in electrons. Same conventions as in Fig. 5.

The interaction with the (BeF₂)₂ dimer implies not only the already mentioned bonding perturbation of the azole moiety but also a bonding perturbation of the (BeF₂)₂ dimer. As can be seen in Fig. 6, the Be interacting with the N atom of the azole is tetracoordinated, so its hybridization is no longer sp^2 but close to sp^3 , the three bonds with the F atoms being weaker than those of the terminal Be atom not interacting with the azole. It is also important to emphasize that the interaction of the (BeF₂)₂ dimer complex with the most basic site of the triazole, N3, does not yield the most stable complex because, as shown in Fig. 6, the association with N2 is favored (-283.5 vs -282.8 kJ mol⁻¹) by the formation of a N1-H...F IMHB. However, the most important finding is that the deprotonation of this global minimum is followed by the formation of a second beryllium bond (Be-N3). In other words, the loss of the proton increases the electron density within the triazole moiety and, accordingly, its intrinsic Lewis basicity, which favors the formation of the new Be-N3 bond, contributes significantly to stabilize the anion. This extra-stabilization implies a further increase in the intrinsic acidity of the triazole moiety of 50 kJ mol⁻¹, which becomes as acidic as the 1H-tetrazole-BeF₂ complex.

The situation is similar when considering the formation of the most stable complex when 1H-tetrazole interacts, through its N4 basic site, with the (BeF₂)₂ dimer (see Fig. 7).

Again, the deprotonation of the tetrazole implies the appearance of a new electron-rich N atom able to interact with the electron-deficient Be atoms, leading to different local minima all of them

stabilized by Be-N interactions (see Fig. S11 of the [supplementary material](#)). However, as in the case of triazoles mentioned above, the global minima correspond always to the interaction with the (BeF₂)₂ dimer because of its enhanced Lewis acidity. This is illustrated by the characteristics of the EDS (see Fig. 8), which show the appearance of two well-defined areas of electron-density accumulation between the N1 and N2 (or N3 and N4) centers of tetrazole anion and the two beryllium bonds.

Consistently, the ELF function shows (see Fig. 9) that whereas the neutral 1H-tetrazol-(BeF₂)₂ complex only exhibits one N4-Be bonding interaction, for the deprotonated species, a second N3-Be (or N2-Be) bonding interaction appears, enhancing the stability of the anion. The obvious consequence is that 1H-tetrazole-(BeF₂)₂ complex is predicted to be 25 kJ mol⁻¹ more acidic than perchloric acid (1255 ± 24 kJ mol⁻¹).⁵⁴

CONCLUDING REMARKS

The acid-base interactions between BeF₂ and triazoles and tetrazoles lead to very stable complexes, which involve a significant bonding perturbation of the two interacting subunits. For BeF₂, the electron density transfer from the azole to the empty p orbitals of Be involves a hybridization change in this center reflected in a F-Be-F angle in the range of 137°–140°. The aforementioned electron density transfer also affects the azole subunit whose intrinsic

acidity increases dramatically, and typical bases become proton donors stronger than conventional acids such as phosphoric or even sulfuric acids. When the interaction involves two BeF_2 , the most stable complex corresponds systematically to the interaction of the azole with the $(\text{BeF}_2)_2$ dimer, which is a Lewis acid much stronger than the monomer because the Be atoms are tricoordinated with F atoms. This is reflected in binding energies with the dimer that is more than double the binding energies with the monomer. Interestingly, although practically in all cases, the azoles under investigation have directly connected N basic sites, the most stable complex with the $(\text{BeF}_2)_2$ dimer is always monodentate. The situation changes completely when the azole subunit becomes deprotonated because the electron density involved in the broken N–H bond is now available to be transferred to the second Be atom of the $(\text{BeF}_2)_2$ dimer, so the global minimum of the deprotonated species is characterized

by the formation of a new $\text{N-N-Be-(F}_2\text{)-Be}$ five-membered ring. The contribution that this additional link makes to the stability of the system renders most of the azole- $(\text{BeF}_2)_2$ complexes investigated to be stronger nitrogenous acids than oxyacids such as perchloric acid.

All in all, the perturbation caused by the beryllium bonds in the acidity of the azoles is a new proof that the nature of the bonds responsible for a given chemical property can be strongly altered by non-covalent interactions. This is a general reminder that, although considered as weak interactions, non-covalent interactions might change significant properties that we usually rationalize by paying attention only to the covalent framework of the isolated system.

SUPPLEMENTARY MATERIAL

See [supplementary material](#) for the comparison between B3LYP and ω B97XD optimized geometries for several azoles and their complexes with BeF_2 (Fig. S1), BeF_2 binding enthalpies for some azole- BeF_2 complexes calculated with the G4 method and its G4* modification (Table S1), BeF_2 binding enthalpies for the different complexes between the azoles investigated and BeF_2 (Figs. S2–S10), and optimized structures for alternative local minima of complexes between 1H-tetrazole and two molecules of BeF_2 (Fig. S11).

ACKNOWLEDGMENTS

This work was carried out with financial support from the Ministerio de Ciencia, Innovación y Universidades of Spain (MICIN/AEI) (Grant Nos. 5203125207-25207-4-21 and 5931125495-125495-4-21). The authors also thank the CTI (CSIC) and the Centro de Computación Científica of the UAM (CCC-UAM) for the generous allocation of computer time and for their continued technical support.

AUTHOR DECLARATIONS

Conflict of Interest

The authors have no conflicts to disclose.

Author Contributions

All authors contributed equally to this work.

DATA AVAILABILITY

The data that support the findings of this study are available within the article and its [supplementary material](#).

REFERENCES

- 1 C. A. Coulson, *Valence* (Clarendon Press, Oxford, 1953).
- 2 I. Cukrowski, "A unified molecular-wide and electron density based concept of chemical bonding," *Wiley Interdiscip. Rev.: Comput. Mol. Sci.* **2021**, e1579.
- 3 P. Ball, "Beyond the bond," *Nature* **469**, 26–28 (2011).
- 4 R. Balawender, F. De Proft, and P. Geerlings, "Nuclear Fukui function and Berlin's binding function: Prediction of the Jahn-Teller distortion," *J. Chem. Phys.* **114**, 4441–4449 (2001).
- 5 D. Chakraborty *et al.*, "Understanding chemical binding using the Berlin function and the reaction force," *Chem. Phys. Lett.* **539**, 168–171 (2012).
- 6 R. K. Carlson, D. G. Truhlar, and L. Gagliardi, "On-top pair density as a measure of left-right correlation in bond breaking," *J. Phys. Chem. A* **121**, 5540–5547 (2017).
- 7 P. Chaquin and P. Reinhardt, "Deformation forces in promolecules revisited: Binding of homonuclear diatomic molecules and calculation of stretching vibrational frequencies in diatomic and larger systems," *Comput. Theor. Chem.* **1096**, 33–39 (2016).
- 8 I. Alkorta, J. Elguero, and C. Foces-Foces, "Dihydrogen bonds (A–H...H–B)," *Chem. Commun.* **1996**, 1633–1634.
- 9 M. Yáñez *et al.*, "Beryllium bonds, do they exist?," *J. Chem. Theor. Comput.* **5**, 2763–2771 (2009).
- 10 S. Zahn *et al.*, "Pnicogen bonds: A new molecular linker?," *Chem. - Eur. J.* **17**, 6034–6038 (2011).
- 11 A. Bauzá, T. J. Mooibroek, and A. Frontera, "Tetrel-bonding interaction: Rediscovered supramolecular force?," *Angew. Chem., Int. Ed.* **52**, 12317–12321 (2013).
- 12 E. E. Tucker and S. D. Christian, "Hydrogen-bond cooperativity. Methanol-tri-norm-octylamine system in normal-hexadecane," *J. Am. Chem. Soc.* **97**, 1269–1271 (1975).
- 13 O. Mó, M. Yáñez, and J. Elguero, "Cooperative (nonpairwise) effects in water trimers: An *ab initio* molecular orbital study," *J. Chem. Phys.* **97**, 6628–6638 (1992).
- 14 J. Gu, J. Wang, and J. Leszczynski, "Cooperative effects: Stabilization of the isoguanine trimer," *J. Phys. Chem. B* **108**, 8017–8022 (2004).
- 15 O. Mó *et al.*, "Cooperativity and proton transfer in hydrogen-bonded triads," *Chemphyschem* **6**, 1411–1418 (2005).
- 16 S. J. Grabowski and E. Bilewicz, "Cooperativity halogen bonding effect—*Ab initio* calculations on $\text{H}_2\text{CO}\cdots(\text{ClF})_n$ complexes," *Chem. Phys. Lett.* **427**, 51–55 (2006).
- 17 M. Roman *et al.*, "Supramolecular balance: Using cooperativity to amplify weak interactions," *J. Am. Chem. Soc.* **132**, 16818–16824 (2010).
- 18 C. Estarellas *et al.*, "Theoretical study on cooperativity effects between anion- π and halogen-bonding interactions," *Chemphyschem* **12**, 2742–2750 (2011).
- 19 L. Albrecht *et al.*, "Cooperativity between hydrogen bonds and beryllium bonds in $(\text{H}_2\text{O})_n\text{BeX}_2$ ($n = 1-3$, $X = \text{H, F}$) complexes. A new perspective," *Phys. Chem. Chem. Phys.* **14**, 14540–14547 (2012).
- 20 S. J. Grabowski, "Cooperativity of hydrogen and halogen bond interactions," *Theor. Chem. Acc.* **132**, 1347 (2013).
- 21 I. Alkorta *et al.*, "Cooperativity in beryllium bonds," *Phys. Chem. Chem. Phys.* **16**, 4305–4312 (2014).

- ²²J. George, V. L. Deringer, and R. Dronskowski, "Cooperativity of halogen, chalcogen, and pnictogen bonds in infinite molecular chains by electronic structure theory," *J. Phys. Chem. A* **118**, 3193–3200 (2014).
- ²³L. Albrecht and R. J. Boyd, "Atomic energy analysis of cooperativity, anti-cooperativity, and non-cooperativity in small clusters of methanol, water, and formaldehyde," *Comput. Theor. Chem.* **1053**, 328–336 (2015).
- ²⁴M. D. Esrafil, R. Nurazar, and F. Mohammadian-Sabet, "Cooperative effects between tetrel bond and other σ -hole bond interactions: A comparative investigation," *Mol. Phys.* **113**, 3703–3711 (2015).
- ²⁵S. A. C. McDowell and D. S. Hamilton, "Cooperative effects of hydrogen, halogen and beryllium bonds on model halogen-bonded FCl...YZ (YZ = BF, CO, N-2) complexes in FX'...FCl...YZ trimers (FX' = FH, FCl, F₂Be)," *Mol. Phys.* **113**, 1991–1997 (2015).
- ²⁶A. S. Mahadevi and G. N. Sastry, "Cooperativity in noncovalent interactions," *Chem. Rev.* **116**, 2775–2825 (2016).
- ²⁷M. Marin-Luna, I. Alkorta, and J. Elguero, "Cooperativity in tetrel bonds," *J. Phys. Chem. A* **120**, 648–656 (2016).
- ²⁸S. A. C. McDowell and C. S. Fiedler, "A computational study of beryllium-bonded H₂Be...FNgH/FKrCl (Ng = Ar, Kr) dyads and their intermolecular interactions with the model nucleophiles F[−], NH₃ and NCH," *Comput. Theor. Chem.* **1084**, 150–156 (2016).
- ²⁹M. Liu *et al.*, "Modulating the strength of tetrel bonding through beryllium bonding," *J. Mol. Model.* **22**, 192 (2016).
- ³⁰C. Trujillo *et al.*, "Cooperative effects in weak interactions: Enhancement of tetrel bonds by intramolecular hydrogen bonds," *Molecules* **24**(2), 308 (2019).
- ³¹H. Lin *et al.*, "Comparison of pnictogen and tetrel bonds in complexes containing CX₂ carbenes (X = F, Cl, Br, OH, OMe, NH₂, and NMe₂)," *New J. Chem.* **43**, 15596–15604 (2019).
- ³²J. E. Walley *et al.*, "Cyclic(alkyl)(amino) carbene-promoted ring expansion of a carbodicarbene beryllacycle," *Inorg. Chem.* **58**, 11118–11126 (2019).
- ³³M. Hurtado *et al.*, "The ever-surprising boron chemistry. Enhanced acidity of phosphine-boranes," *Chem. - Eur. J.* **15**, 4622–4629 (2009).
- ³⁴O. Mó *et al.*, "Enhancing and modulating the intrinsic acidity of imidazole and pyrazole through beryllium bonds," *J. Mol. Model.* **19**, 4139–4145 (2013).
- ³⁵A. Martín-Sómer *et al.*, "Acidity enhancement of unsaturated bases of group 15 by association with borane and beryllium dihydride. Unexpected boron and beryllium Brønsted acids," *Dalton Trans.* **44**, 1193–1202 (2014).
- ³⁶M. Yáñez *et al.*, "Can conventional bases and unsaturated hydrocarbons be changed into gas-phase superacids stronger than most of the known oxyacids? The role of beryllium bonds," *Chem. - Eur. J.* **19**(35), 11637–11643 (2013).
- ³⁷L. A. Curtiss, P. C. Redfern, and K. Raghavachari, "Gaussian-4 theory," *J. Chem. Phys.* **126**, 084108 (2007).
- ³⁸C. Moller and M. S. Plesset, "Note on an approximation treatment for many-electron systems," *Phys. Rev.* **46**, 618–622 (1934).
- ³⁹R. Krishnan and J. A. Pople, "Approximate fourth-order perturbation-theory of electron correlation energy," *Int. J. Quantum Chem.* **14**, 91–100 (1978).
- ⁴⁰K. Raghavachari *et al.*, "A fifth-order perturbation comparison of electron correlation theories," *Chem. Phys. Lett.* **157**, 479–483 (1989).
- ⁴¹R. F. W. Bader, *Atoms in Molecules: A Quantum Theory* (Clarendon Press, Oxford, 1990).
- ⁴²G. Sánchez-Sanz *et al.*, "Electron density shift description of non-bonding intramolecular interactions," *Comput. Theor. Chem.* **991**, 124–133 (2012).
- ⁴³A. Savin *et al.*, "ELF: The electron localization function," *Angew. Chem., Int. Ed.* **36**(17), 1809–1832 (1997).
- ⁴⁴I. Iribarren *et al.*, "Evaluation of electron density shifts in noncovalent interactions," *J. Phys. Chem. A* **125**, 4741–4749 (2021).
- ⁴⁵G. W. Frisch *et al.*, Gaussian 16, Revision C.01, Gaussian, Inc., Wallingford, CT, 2016.
- ⁴⁶T. Lu and F. Chen, "Multiwfn: A multifunctional wavefunction analyzer," *J. Comput. Chem.* **33**, 580–592 (2012).
- ⁴⁷See <http://www.jmol.org/> for Jmol: an open-source Java viewer for chemical structures in 3D.
- ⁴⁸J. Catalán *et al.*, "The azoles—A theoretical study," *Chem. Scripta* **24**, 84–91 (1984).
- ⁴⁹J.-L. M. Abboud *et al.*, "Basicity of N-H- and N-methyl-1,2,3-triazoles in the gas phase, in solution, and in the solid state—An experimental and theoretical study," *Eur. J. Org. Chem.* **2001**, 3013–3024.
- ⁵⁰Note that in Fig. 2, we provide the negative value of the PA, which is usually defined as the enthalpy of the deprotonation reaction $AH^+ \rightarrow A + H^+$.
- ⁵¹R. A. Morris *et al.*, "The gas-phase acidity of H₃PO₄," *J. Chem. Phys.* **106**, 3545 (1997).
- ⁵²J. A. Davidson, F. C. Fehsenfeld, and C. J. Howard, "The heats of formation of NO₃[−] and NO₃[−] association complexes with HNO₃ and HBr," *Int. J. Chem. Kinet.* **9**, 17 (1977).
- ⁵³X.-B. Wang, J. B. Nicholas, and L.-S. Wang, "Photoelectron spectroscopy and theoretical calculations of SO₄[−] and HSO₄[−]: Confirmation of high electron affinities of SO₄ and HSO₄," *J. Phys. Chem. A* **104**, 504–508 (2000).
- ⁵⁴M. M. Meyer and S. R. Kass, "Experimental and theoretical gas-phase Acidities, bond dissociation energies, and heats of formation of HClO_x, x = 1–4," *J. Phys. Chem. A* **114**, 4086–4092 (2010).